EUROPHYSICS LETTERS 1 May 2006

Europhys. Lett., **74** (3), pp. 452–458 (2006)
DOI: 10.1209/epl/i2005-10550-y

Mechanism of discrete breather excitation in driven micro-mechanical cantilever arrays

P. Maniadis and S. Flach

Max-Planck-Institut für Physik Komplexer Systeme
Nöthnitzer Str. 38, D-01187 Dresden, Germany

received 2 July 2005; accepted in final form 1 March 2006
published online 29 March 2006

PACS. 63.20.Pw – Localized modes.
PACS. 05.45.Xt – Synchronization; coupled oscillators.
PACS. 05.45.-a – Nonlinear dynamics and nonlinear dynamical systems.

Abstract. – We study the pathway of generating discrete breathers in damped and driven micromechanical cantilever arrays. Using the concept of the nonlinear response manifold we provide a systematic way to find the optimal parameter regime in damped and driven lattices where discrete breathers exist. Our results show that discrete breathers appear via a new instability of the manifold, different from the anticipated modulational instability known for conservative systems. We present several ways of exciting breathers, and compare also to experimental studies in antiferromagnetic layered systems.

The existence and the properties of intrinsic localized modes (ILMs) or discrete breathers (DBs) in nonlinear lattices have been investigated thoroughly during the last years (see [1] and references therein). Existence proof confirms that these localized modes are exact solutions in systems of coupled anharmonic oscillators [2]. Numerical techniques have been developed starting from the anticontinuous limit, for the study of the existence and the stability of DBs [1, 3]. Under certain conditions they can become mobile if they are perturbed in the appropriate direction in the phase space [4].

In addition, an impressive number of various experiments during the last years have verified the existence of these modes in many systems like micro-mechanical cantilever arrays [5, 6], antiferromagnets [7–9], Josephson junction arrays [10, 11], coupled optical waveguides [12, 13] atomic vibrations of highly nonlinear materials [14–16] and Bose-Einstein condensates on optical lattices [17].

The bulk of the central theoretical results has been achieved for conservative systems. One good reason for that is the complexity of the DB properties. While DBs typically persist under the influence of weak dissipation (which should also include an energy pumping mechanism), various realisations of dissipation (dc driving, ac driving, fluctuations, linear *vs.* nonlinear damping etc.) modify DB properties in a specific way, turning the limiting conservative case into an ideal starting playground for setting a coherent frame of the understanding of their properties. Since most of the experimental studies face dissipation, each case may call for a specific additional theoretical study.

DB observation in cantilever arrays [5,6] and antiferromagnets [7–9] involved the excitation of the system with spatially homogeneous external fields, triggering a spatially inhomogeneous system state via some inherent instability. For conservative systems the modulational instability (MI) of band edge plane waves is known to provide such a path. Especially for the case

of driven cantilevers, the MI approach for conservative systems was used to design an experimental system of alternating short and long cantilevers [5, 6]. The results we present below show that DBs appear via a completely different instability. We demonstrate that by exciting DBs in arrays with identical cantilever length, which would be impossible following the MI argumentation. The reason is that the spatially uniform external field inherits its uniformity onto the dynamics of the cantilevers regardless of the internal structure. Especially the field can generate frequency-phase oscillations, which are not existing in the absence of the field.

In order to study the driven cantilever system we use the model equations in [5, 6] and introduce the dimensionless time $t \to t/t_0$ and displacement $x_l \to x_l/a_0$, where t_0 and a_0 correspond to a characteristic time and length of the system. The equations of motion describing the cantilever system can be then written as a system of coupled anharmonic damped and ac driven oscillators

$$\ddot{x}_l + \gamma \dot{x}_l + a_2 x_l + a_4 x_l^3 - C(x_{l+1} + x_{l-1} - 2x_l) = A(t). \tag{1}$$

The oscillator displacements x_l describe the deflection angle of the l-th cantilever from its equilibrium position. The hard-type anharmonicity tends to increase the oscillation frequencies with growing amplitudes. This model neglects the influence of longer than nearest-neighbor interactions, which is not crucial for the understanding of the main qualitative DB properties. The dimensionless parameters are related with the ones of the experiment in refs. [5, 6]: $\gamma = t_0/\tau$, $a_2 = k_2 t_0^2/m$, $a_4 = k_4 t_0^2 a_0^2/m$, $C = k_l t_0^2/m$ and $A = \alpha t_0^2/a_0$. Using the experimental values in [5, 6] and setting $a_2 = a_4 = 1$, we find $t_0 = 1.34238 \cdot 10^{-6}$ s and $a_0 = 2.46 \cdot 10^{-5}$ m. The friction and coupling parameters become $\gamma = 1.534 \cdot 10^{-4}$ and $C = 0.07953$. The spatially uniform ac driving $A(t)$ in (1) is generated by a piezoelectric crystal vibration in the original experiments.

Neglecting the damping γ, the ac driving $A(t)$ and the nonlinear force terms in (1) one readily derives the only possible solutions, namely plane waves $x_l \sim \mathrm{e}^{i(\omega_q t - ql)}$ with the linear dispersion relation $\omega_q = \sqrt{1 + 4C \sin^2(q/2)}$ relating the plane-wave frequency ω_q to its corresponding wave number q. Reinstating the nonlinear force terms in (1) leads to two conclusions [1]: i) discrete breathers, *i.e.* time-periodic and spatially localised solutions $x_l(t) = x_l(t + T_b)$, $x_{|l|\to\infty} \to 0$ exist for frequencies $\Omega_b = \frac{2\pi}{T_b} > \omega_{q=\pi}$; ii) the $q = \pi$ plane-wave mode turns (modulationally) unstable at amplitudes $\sim 1/N$, where N is the number of cantilevers, and DBs bifurcate from this plane-wave mode along this very instability route. What can we expect if both damping and ac driving are added as well? DBs persist without much change, thus the ac driving frequency choice $\omega_d > \omega_{q=\pi}$ is well reasoned. However, instabilities of conservative systems may turn sensitive to effects of damping. Assuming that the MI of the staggered $q = \pi$ mode is the track to follow, the choice of a nonstaggered ac driving is not appropriate. Note that the experimental design of alternating short and long cantilevers splits the spectrum ω_q into two bands separated by a gap. In addition it formally transforms the $q = \pi$ mode of the system with identical cantilevers into the $q = 0$ mode of the upper band for the system with alternating cantilever lengths. Yet the staggered character of this mode is of course preserved inside each unit cell which contains now two neighboring cantilevers. Thus the mismatch between the staggered MI mode and the nonstaggered ac driving remains also for systems with alternating cantilever length.

With the above parameters $1 \leq \omega_q \leq 1.1481$. The narrowness of the band as compared to the characteristic frequency values is due to the weak coupling constant C. Let us start then from the uncoupled limit. In that case each oscillator evolves independently. Assuming for the moment small amplitudes of all oscillators, the presence of a weak driving will (after some transient time) bring them all into a unique oscillatory state, thus all oscillators will move

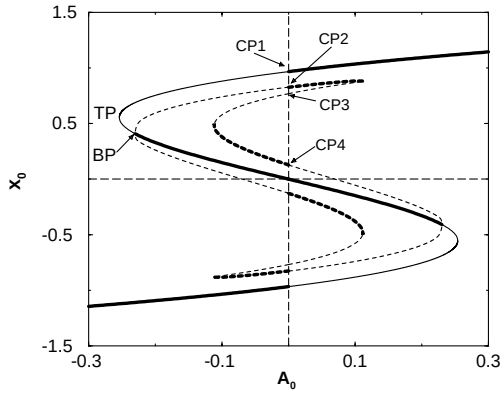

Fig. 1 – The nonlinear response manifold (NLRM) for $C = 0.0079$ and $\omega_d = 1.3$. Solid line: homogeneous branch; dashed line: various breather branches for $x_{0,0}$. Thick lines correspond to stable parts of the manifold; thin lines: to unstable ones. Long-dashed lines correspond to the zero $x_{0,0}$ and A_0 axes.

in phase (with each other). Consequently, we have to study the stability of a *nonstaggered* extended time-periodic state for weak coupling as well, no matter whether the frequency of the driving is located above or below the band ω_q.

For a periodic driving of the form $A(t) = A_0 \cos(\omega_d t)$, eq. (1) supports periodic solutions. It is easier to study first the properties of these solutions at zero friction ($\gamma = 0$), and then examine the modifications when $\gamma \neq 0$. Newton method [1, 3] was used for the tracking of periodic solutions with frequency equal to the external driving of the form: $x_l(t) = x_{0,l} \cdot f(\omega_d t)$ where $x_{0,l}$ is the amplitude of the oscillation, and $f(\omega_d t)$ is a periodic function with period 2π. The Newton scheme was initiated with a very small driving amplitude ($A_0 \simeq 0$), and the response of the system (*i.e.* the amplitude of the oscillations $x_{0,l}$) was followed as A_0 was varying. Thus we reconstruct the full Nonlinear Response Manifold (NLRM) [18]. The main features of the NLRM are shown in fig. 1 for a driving frequency $\omega_d = 1.3$.

The NLRM close to the origin follows from linearising the equation of motion (1). The exact solution of the system in this limit is $x_l(t) = x_{0,l} \cos(\omega_d t)$ with $x_{0,l} = -A_0/(\omega_d^2 - 1)$ (this is a straight line with slope $s = -1/(\omega_d^2 - 1)$). This is a homogeneous branch (HB) (all the oscillators are in phase). There is a phase difference of $\phi = \pi$ between the driving and the response of the system. The NLRM is symmetric around the origin due to $x_l(t + \pi/\omega_d) = -x_l(t)$ and $A(t + \pi/\omega_d) = -A(t)$. Due to this symmetry, for each branch of the manifold with positive $x_{0,0}$, there exists the equivalent branch corresponding to the negative values (with the appropriate change in the sign of A_0). These branches correspond to the same solution but translated by half a period in time.

Increasing $|A_0|$, the displacement $x_{0,0}$ of HB increases, up to the first turning point (TP) (fig. 1) (the use of the absolute value of A_0 is because we refer to the distance from the origin). After the turning point $x_{0,0}$ continues to increase, while the driving amplitude decreases down to zero at the first crossing point (CP1). This crossing point corresponds to a homogeneous solution with all the oscillators oscillating with the same amplitude $x_{0,0}$ and zero driving. This is a stable periodic solution with period equal to the driving period, and it exists due to the frequency increasing, hard anharmonicity term in the equations of motion and because $\omega_d > \omega_q$. The NLRM manifold of the HB continues further from CP1 with again nonzero A_0, but the solution is now in phase with the driving.

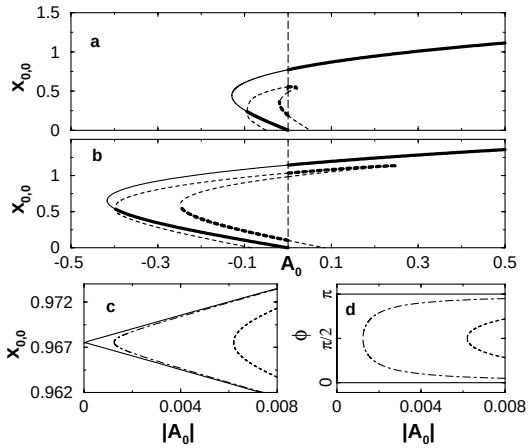

Fig. 2 – (a, b) The NLRM for different values of the driving frequency: (a) $\omega_d = 1.2$, (b) $\omega_d = 1.4$. The parameters are the same used in fig. 1. (Thick lines correspond to stable parts of the manifold, thin lines to unstable ones.) (c, d) The response $x_{0,0}$ and the phase difference ϕ of the manifold in the neighborhood of the first crossing point for different values of the friction. The continuous line corresponds to $\gamma = 0$, the dashed-dotted line to $\gamma = 0.001$ and the dashed line to $\gamma = 0.005$. The long-dashed line in (a) and (b) corresponds to the zero A_0 axis.

The Floquet stability analysis [1] of the HB reveals that close to the origin the manifold is linearly stable. An instability appears before the TP and the HB becomes unstable. The homogeneous branch remains unstable between the TP and the CP1. After the CP1, the homogeneous branch turns stable again (see fig. 1).

The instabilities of the HB mark the bifurcation of spatially inhomogeneous solutions —various breather states— of the HB. This point is labeled as BP in fig. 1. For a system of N oscillators, at the first instability, N new branches of the NLRM appear. Each of these branches correspond to a single breather centered at a different site on the lattice. In fig. 1 we show two of these branches with dashed lines bifurcating from the homogeneous solution at the bifurcation point BP. Starting from the bifurcation, the displacement of the central oscillator increases, while $|A_0|$ decreases. For $A_0 = 0$ the manifold passes through the second crossing point (CP2). This branch of the manifold corresponds to a breather, and is stable for $A_0 > 0$ and unstable for $A_0 < 0$. After that, the manifold turns, and passes through further crossing points. Thus for fixed ω_d we have multistability for small enough A_0 with a large-amplitude and a small-amplitude HB coexisting together with breather states. For large enough A_0 only the large-amplitude HB survives.

The NLRM depends on the driving frequency ω_d. In fig. 2 (a and b) we show a part of the NLRM for two different values of the driving frequency. In fig. 2(a) $\omega_d = 1.2$ and in fig. 2(b) $\omega_d = 1.4$. With increasing frequency the slope of the manifold decreases, the crossing points appear for larger values of $x_{0,0}$; as a result, the bifurcation and the turning points appear for larger values of $|A_0|$.

The properties of the manifold are slightly modified due to the presence of friction ($\gamma \neq 0$). The NLRM between the origin and the crossing point (CP1) for $\gamma = 0$ is in anti-phase with the driver, while after the crossing point the NLRM is in phase with the driver. For $\gamma = 0$ therefore there is a phase difference of $\phi = \pi$ in the response of the system around a CP. When a small friction is introduced in the system, it creates an extra small phase difference between the driver and the response. This phase difference between the driver and the response increases

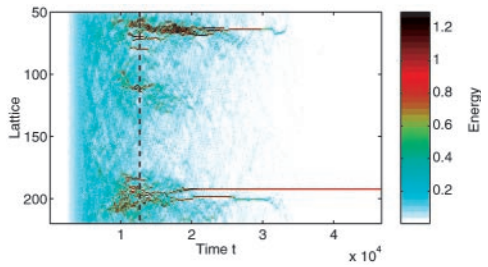

Fig. 3 – Energy density as a function of time and space. The driving frequency is initially ramped from $\omega_d = 1.14$ to $\omega_d = 1.4$, and then it remains fixed (marked by the vertical dashed line). Energy pumping is observed during the ramping. At the end of the ramping process, breathers are created, and one of them locks to the driving and survives.

in the neighborhood of the CP. As a result, the solution at the CP disappears due to friction, but there is a smooth transition between the two different branches of the manifold. The phase difference ϕ varies smoothly from $\pi - \epsilon_-$ to $0 + \epsilon_+$, where $\epsilon_\pm$ correspond to the small phase differences created by the friction on the large- and small-amplitude branch, respectively, far from the CP. For weak damping this transition occurs very close to the CP. The smooth transition between the two branches of the manifold in the neighborhood of (CP1) as a function of $|A_0|$ is shown in fig. 2(c) for different values of the friction. The smooth transition in the phase difference ϕ is shown in fig. 2(d). Far from the CP, the properties of the manifold are only slightly modified by the nonzero friction.

As follows from fig. 1 and fig. 2 (a and b), the stable breather branch is not connected to the stable HB of the NLRM. Thus we can exclude an easy way of exciting the system in the HB and tuning some parameter (amplitude or frequency of the driving) such that we continuously join the breather branch. This calls for stochastic excitations of the system to enforce a nonzero probability to end up in a breather state when initially starting from a HB. Similar to the experiments [5,6] we performed a ramping of the frequency ω_d from 1.14 (inside the band) to 1.4 (above the band) for fixed amplitude $A_0 = 0.008$ (cf. fig. 4(b)). According to fig. 2, the final state corresponds to the multistability domain of the NLRM. If the system was initially at rest, the final state is observed to be the small-amplitude HB. However, if we consider some random initial conditions for the cantilever deflection angles, uniformly distributed in the interval $(-0.05, 0.05)$, the ramping process excites a finite-time energy pumping (fig. 3). During the pumping period, the oscillation amplitudes of the cantilevers are amplified and regions of large-amplitude oscillations are created. After the ramping finishes, most of these large-amplitude oscillations decay back into the low-amplitude HB, while some of them may lock to the driver and turn into a stable breather. The average energy per oscillator is shown in fig. 4(a) as a function of time (line 1). During the ramping, there is a frequency window, where energy is pumped into the system, and then the system relaxes due to dissipation. Line 2 shows the energy of the locked breather site.

The creation of large-amplitude oscillations can also be observed in the absence of frequency ramping, when the randomness in the initial displacements is stronger. If we perform simulations in the absence of a frequency ramping, but with larger fluctuations in the distribution of initial displacements (Gaussian distribution of initial displacements with zero mean and variance $D = 0.5$) we observe again large-amplitude oscillations which can lock into stable breathers or decay. Keeping the frequency and the driving amplitude fixed ($\omega_d = 1.4$ and $A_0 = 0.008$) we observe the creation and locking of breathers similar to the locked breathers

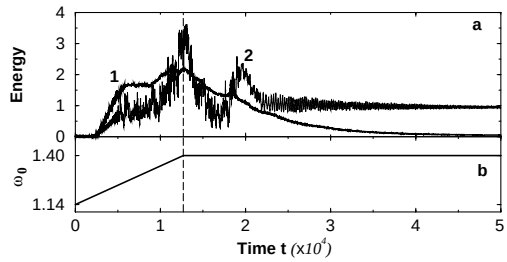

Fig. 4 – (a) Average energy per oscillator as a function of time (line 1, scaled by a factor of 10 for better observation) and the energy of the locked oscillator (line 2). The parameters and the frequency ramping are as in fig. 3. (b) The frequency ramping scheme. After the vertical dashed line the driving frequency remains constant.

found in fig. 3. The behavior of the system is similar when we perform simulations in a system with alternating long and short cantilevers.

The NLRM can be also used to study the breather excitation in antiferromagnetic systems [7,8] where external driving was used as well. The observed breather destruction in these experiments is similar to the process presented in fig. 5. In analogy with the experiment a strong driving at frequency $\omega_1 = 1.8$ with $A_1 = 0.8$ and duration of $t = 698.1$ is used, together with initial displacements being uniformly distributed in the interval $(-0.25, 0.25)$. As a result, a DB is formed (fig. 5(a)). A subsequent long driving at a frequency $\omega_2 = 1.4$ (being located closer to the spectrum ω_q) is exciting the system with a small amplitude $A_2 = 0.008$. Because of the frequency mismatch the breather with ω_1 will start to decay, but tend to slow down the decay when its frequency is close to ω_2 (fig. 5(c)). Similarly to the experimental case we add a third weak driving signal with $\omega_3 = 2$ and amplitude $A_3 = 0.0004$. That hinders the locking of the DB to ω_2. Right after the DB frequency passes ω_2, its relaxation speeds up and the excitation is destroyed very quickly (fig. 5(b), cf. also fig. 3 in [7]. The observed energy release is fixed by the energy value of a DB locked to the ω_2 driving and explains the experimental observation of equal height steps in the relaxation of DBs. At the same time we

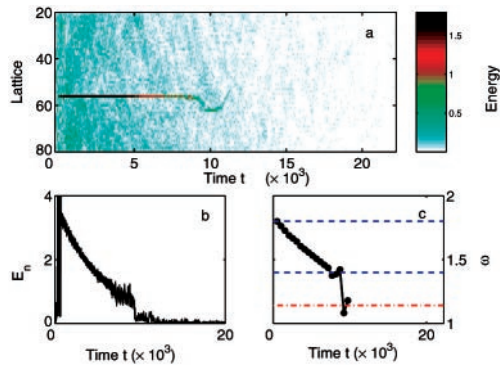

Fig. 5 – (a) Energy density evolution for a sequence of different driving (see text for details); (b) time dependence of the DB energy observed in (a); (c) time dependence of the DB frequency observed in (a). The two dashed lines mark the frequencies ω_1 and ω_2. The dash-dotted line corresponds to band edge frequency ω_π.

interpret the observed smooth decrease of the emission signal in fig. 3 in [7] as a process of slow relaxation of DBs with frequency ω_1 towards DBs with frequency ω_2.

The NLRM study shows that breathers can be obtained in a driven and damped system by carefully choosing the frequency (outside the phonon band) and amplitude of the driving force (not being too large) such that the NLRM is activated inside the multistability domain. We have shown that localised breathers emerge from the homogeneous solution via an instability of the NLRM completely different from the expected MI picture. The fact that the stable breather branch is disconnected from the stable HB, implies that one needs random perturbations in the initial conditions in order to perform a crossover from one to the other. There exist various pathways of generating breathers, either by frequency ramping which causes energy pumping or by initially strongly exciting the system with random displacements. These pathways have to be designed in such a way that the system will tend to the small-amplitude HB of the NLRM, with some fluctuations growing locally into large-amplitude oscillations, which finally transform into breather states.

* * *

We thank A. J. Sievers and U. Schwartz for helpful discussions.

REFERENCES

[1] Aubry S., *Physica D*, **103** (1997) 201; Flach S. and Willis C. R., *Phys. Rep.*, **295** (1998) 181; Dauxois T., Litvak-Hinenzon A., MacKay R. and Spanoudaki A. (Editors), *Energy Localisation and Transfer* (World Scientific, Singapore) 2004; Campbell D. K., Flach S. and Kivshar Yu. S., *Phys. Today*, issue no. 1, **57** (2004) 43.
[2] MacKay R. S. and Aubry S., *Nonlinearity*, **7** (1994) 1623.
[3] Marin J. L. and Aubry S., *Nonlinearity*, **9** (1994) 1501.
[4] Chen Ding, Aubry S. and Tsironis G. P., *Phys. Rev. Lett.*, **77** (1996) 4776.
[5] Sato M., Hubbard B. E., Sievers A. J., Ilic B., Czaplewski D. A. and Craighead H. G., *Phys. Rev. Lett.*, **90** (2003) 044102.
[6] Sato M., Hubbard B. E., English L. Q., Sievers A. J., Ilic B., Czaplewski D. A. and Craighead H. G., *Chaos*, **13** (2003) 702; Sato M., Hubbard B. E. and Sievers A. J., *Rev. Mod. Phys.*, **78** (2006) 137.
[7] Sato M. and Sievers A. J., *Nature*, **432** (2004) 486.
[8] Sato M. and Sievers A. J., *Phys. Rev. B*, **71** (2005) 214306.
[9] Schwarz U. T., English L. Q. and Sievers A. J., *Phys. Rev. Lett.*, **83** (1999) 223.
[10] Trias E., Mazo J. and Orlando T., *Phys. Rev. Lett.*, **84** (2000) 741.
[11] Binder P., Abraimov D., Ustinov A. V., Flach S. and Zolotaryuk Y., *Phys. Rev. Lett.*, **84** (2000) 745.
[12] Fleischer J. W., Segev M., Efremidis N. K. and Christodoulides D. N., *Nature*, **422** (2003) 147.
[13] Eisenberg H. S., Silberberg Y., Morantotti R., Boyd A. R. and Atchinson J. S., *Phys. Rev. Lett.*, **81** (1998) 3383.
[14] Swanson B. I., Brozik J. A., Love S. P., Strouse G. F., Shreve A. P., Bishop A. R., Wang W. Z. and Salkola M. I., *Phys. Rev. Lett.*, **82** (1999) 3288.
[15] Edler J., Hamm P. and Scott A. C., *Phys. Rev. Lett.*, **88** (2002) 067403.
[16] Edler J. and Hamm P., *J. Chem. Phys.*, **117** (2002) 2415.
[17] Eiermann B., Anker Th., Albiez M., Taglieber M., Treutlein P., Marzlin K. P. and Oberthaler M. K., *Phys. Rev. Lett.*, **92** (2004) 230401.
[18] Kopidakis G. and Aubry S., *Physica D*, **130** (1999) 155; **139** (2000) 247; *Phys. Rev. Lett.*, **84** (2000) 3236.